Research Article | Vol. 8, No. 7 | 1 Jul 2018 | OPTICAL MATERIALS EXPRESS 1968
Optical Materials EXPRESS

Machinable ceramic for high performance and compact THz optical components

ANDREAS K. KLEIN,[1,2,*] JONATHAN HAMMLER,[1,2] CLAUDIO BALOCCO,[1] AND ANDREW J. GALLANT[1]

[1]*Department of Engineering, Durham University, South Road, DH1 3LE, Durham, UK*
[2]*These two authors contributed equally*
**andreas.klein@durham.ac.uk*

Abstract: The properties of Shapal Hi-M Soft, an aluminum nitride based ceramic, as a material for THz optical components are investigated and compared with other ceramic materials. Shapal is a low-cost and machinable ceramic with a high-refractive index and low losses at THz frequencies: n = 2.65, α = 0.4 cm^{-1}. To demonstrate the shaping capabilities, a Fresnel lens is fabricated with a micro-milling system. Additionally, a prism as an example of a bulk component is demonstrated. Both a THz time domain spectrometer and a vector network analyzer (0.75–1.1 THz) are used for the optical characterization and the absorption coefficient is precisely obtained in the VNA frequency range.

OCIS codes: (160.2750) Glass and other amorphous materials; (160.4670) Optical materials; (160.4760) Optical properties; (350.3850) Materials processing; (300.6495) Spectroscopy, terahertz.

References and links

1. D. Grischowsky, S. Keiding, M. van Exter, and Ch. Fattinger, "Far-infrared time-domain spectroscopy with terahertz beams of dielectrics and semiconductors," J. Opt. Soc. B **7**(10), 2006–2015 (1990).
2. B. Morgan, C. M. Waits, J. Krizmanic, and R. Ghodssi, "Development of a deep silicon phase fresnel lens using gray-scale lithography and deep reactive ion etching," J. Microelectromech. Syst. **13**(1), 113–120 (2004).
3. D. Seliuta, I. Kasalynas, V. Tamosiunas, S. Balakauskas, Z. Martunas, S. Asmontas, G. Valusis, A. Lisauskas, H. G. Roskos, and K. Kohler, "Silicon lens-coupled bow-tie InGaAs-based broadband terahertz sensor operating at room temperature," Electron. Lett. **42**(14), 825 (2006).
4. D. F. Filipovic, S. S. Gearhart, and G. M. Rebeiz, "Double-slot antennas on extended hemispherical and elliptical silicon dielectric lenses," IEEE Trans. Microw. Theory Tech. **10**(7), 1738–1749 (2000).
5. E. D. Walsby, S. M. Durbin, D. R. S. Cumming, and R. J. Blaikie, "Analysis of silicon terahertz diffractive optics," Curr. Appl. Phys. **4**(2-4), 102–105 (2004).
6. S. Wietzke, C. Jansena, M. Reutera, T. Junga, D. Kraft, S. Chatterjee, B. M. Fischer, and M. Koch, "Terahertz spectroscopy on polymers: A review of morphological studies," J. Mol. Struct. **1006**(1-3), 41–51 (2011).
7. B. Ng, J. Wu, S. M. Hanham, A. I. Fernández-Domínguez, N. Klein, Y. F. Liew, M. B. H. Breese, M. Hong, and S. A. Maier, "Spoof plasmon surfaces: a novel platform for THz sensing," Adv. Opt. Mater. **1**(8), 543–548 (2013).
8. B. Scherger, C. Jördens, and M. Koch, "Variable-focus terahertz lens," Opt. Express **19**(5), 4528–4535 (2011).
9. M. Naftaly, P. J. Greenslade, R. E. Miles, and D. Evans, "Low loss nitride ceramics for terahertz windows," Opt. Mater. **31**(11), 1575–1577 (2009).
10. K. Z. Rajab, M. Naftaly, E. H. Linfield, J. C. Nino, D. Arenas, D. Tanner, R. Mittra, and M. Lanagan, "Broadband dielectric characterization of aluminum oxide (Al_2O_3)," J. Micro. And Elect. Pack. **5**, 101–106 (2008).
11. P. Samoukhina, S. Kamba, S. Santhi, J. Petzelt, M. Valant, and D. Suvorov, "Infrared and terahertz dielectric spectra of novel Bi_2O_3–Nb_2O_5 microwave ceramics," J. Eur. Ceram. Soc. **25**(12), 3085–3088 (2005).
12. J. B. Huang, B. Yang, C. Y. Yu, G. F. Zhang, H. Xue, Z. X. Xiong, G. Viola, R. Donnan, H. X. Yan, and M. J. Reece, "Microwave and terahertz dielectric properties of $MgTiO_3$–$CaTiO_3$ ceramics," Mater. Lett. **136**(1), 225–227 (2015).
13. M. K. Gunde and M. Macek, "Infrared optical constants and dielectric response functions of silicon nitride and oxynitride films," Phys. Status Solidi, A Appl. Res. **183**, 439 (2001).
14. D. Y. Smith, E. Shiles, and M. Inokuti, *Handbook of Optical Constants of Solids* (Chestnut Hill, 1998), pp. 306–406.

#330575 https://doi.org/10.1364/OME.8.001968
Journal © 2018 Received 30 Apr 2018; revised 15 Jun 2018; accepted 15 Jun 2018; published 26 Jun 2018

Optical Materials EXPRESS

15. Z.-M. Huang, J.-G. Huang, Y.-Q. Gao, Yu. M. Andreev, D. M. Ezhov, and V. A. Svetlichnyi, "Optical properties of vanadium and nitrogen doped 4H and 6H-SiC," in *IEEE Proc. of 18th Int. Conf. of Young Specialists on Micro/Nanotechnologies and Electron Devices EDM* (2017).
16. M. Naftaly, J. F. Molloy, B. Magnusson, Y. M. Andreev, and G. V. Lanskii, "Silicon carbide-a high-transparency nonlinear material for THz applications," Opt. Express **24**(3), 2590–2595 (2016).
17. J. Hammler, A. J. Gallant, and C. Balocco, "Free-space permittivity measurement at terahertz frequencies with a vector network analyser," IEEE Trans. Terahertz Sci. Technol. **6**(6), 817–823 (2016).
18. M. Naftaly, "An international intercomparison of THz time-domain spectrometers," in *41st IRMMW-THz Conference* (2016).
19. Precision Ceramics, "Machinable ceramic - chemical composition and thermal conductivity of shapal-m machinable ceramic from precision ceramics", datasheet (2008).
20. Precision Ceramics, "Macor - A Unique Material", datasheet (2016).
21. A. Podzorov and G. Gallot, "Low-loss polymers for terahertz applications," Appl. Opt. **47**(18), 3254–3257 (2008).
22. E. Hecht, *Optics*, 2nd ed. (Addison Wesley, 1987).

1. Introduction

Currently used THz optics can be classified as either high performance, such as high-resistivity float-zone (HRFZ) silicon or low cost e.g. HDPE, UHMWPE, wax polymers, etc. While HRFZ-Si has very low absorption and a high refractive index [1], it is also expensive, brittle and requires elaborate and expensive techniques to produce complex shapes [2]. Therefore, whilst silicon lenses are commonly used, e.g. in THz Time-Domain Spectroscopy systems (THz-TDS) [3], the limited shaping capabilities usually require some adjustment to the components, e.g. using a stack of wafers as spacer [4] or many processing steps if semiconductor manufacturing is used [5]. Conversely, the low-cost materials that can be readily shaped using traditional subtractive manufacturing techniques, in addition to 3D-printing, also have a low refractive index ($n \approx 1.2–1.8$ [6]) which results in less compact optical components. Such materials are also not very resilient to being scratched or exposed to large temperature ranges, making them less suitable for some real world applications. Wax materials have only been successfully used in laboratory environments [7] with, bulky high dynamic range measurement systems, e.g. THz-TDS, which can overcome significant losses within the optical components. Similarly, the use of more exotic components, e.g. based on oil, which has good optical properties at THz frequencies, will probably remain limited to laboratory environments due to practicality issues [8].

Here we present an alternative material option, an aluminum-nitride (AlN) based ceramic, tradename Shapal Hi-M Soft, which is shown to have a relatively high refractive index ($n = 2.65$) within the THz region, reasonably low losses, and is compatible with standard subtractive manufacturing technologies, making it suitable for high performance, compact optics. Additionally, the low absorption and high refractive index make Shapal an interesting alternative material for traditional components, where even fundamental components like prisms made of HRFZ-Si often cost thousands of USD could be offered for a fraction of the price when made from a ceramic alternative. The ceramic will be compared to commonly used materials for THz optics, i.e. HRFZ-Si and polymers, and other ceramics with regards to the refractive index, optical losses and shaping capabilities. As for the shaping capabilities, we focus on machinability using general purpose tools and machinery, as this is the most commonly available method of fabrication. Furthermore, avoiding highly specialized manufacturing techniques is most likely necessary for a material to have commercial success.

Optical Materials EXPRESS

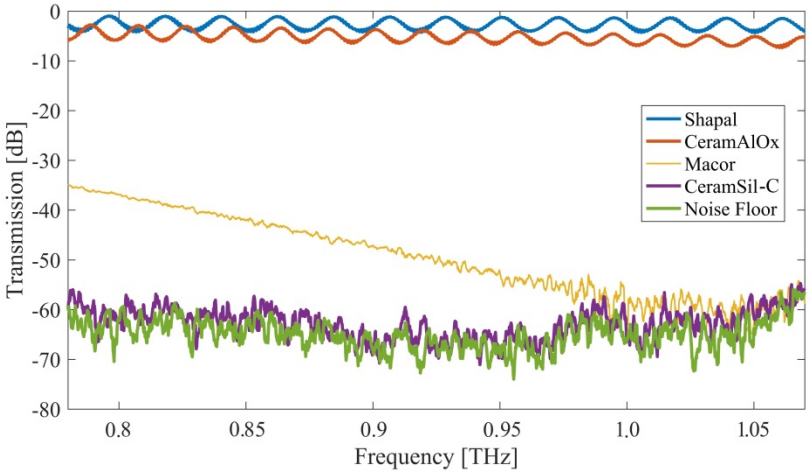

Fig. 1. THz transmission of the ceramics listed in Table 1. Both Macor and CeramSil exhibit very high losses in this region, and there is no measurable transmission through silicon carbide Shapal and CeramAlOx both exhibit low absorption in the frequency range around 1 THz. Sample thickness for all materials was 2.54 mm.

2. Material characterization

Ceramics have attracted some interest as materials for THz optics in the past [9–12]. Therefore, the investigation of other low-cost, machinable alternatives appears to be a natural step. Here we compare two machinable ceramics; Shapal (nitride based) and Macor (oxide based), with two non-machinable ceramics; silicon carbide (SiC, tradename: CeramSil-C) and aluminum oxide (tradename: CeramAlOx). These materials are outlined in Table 1.

As Fig. 1 shows, Shapal exhibits the highest transmission of the above listed materials, making it, in combination with its shaping capabilities, an ideal candidate for THz optical components. The performance of Macor, the other machinable ceramic, is low because it is based on SiO_2 which is known to have significant absorption at THz frequencies [13-14]. The SiC based ceramic, CeramSil, shows no transmission at all. A direct comparison with literature is difficult, as SiC has not been studied in a ceramic form at THz frequencies and, in a crystalline form, many different polymorphs exist. There are reports of high absorption for some polymorphs [15], when they are doped, but there are also reports of attenuation coefficients below 1 cm^{-1} [16]. While CeramSil has very high absorption at THz frequencies, a SiC ceramic made of a high grade low attenuation polymorph may still be a good choice as a THz material, but is not as easy to machine as Shapal.

The refractive indices for Shapal and CeramAlOx, as shown in Table 1, have been determined with the method described in [17] with a Keysight N5224A Vector Network Analyzer (VNA) and VDI THz frequency extenders (WR1.0). The attenuation coefficient, α, was determined by measuring the transmission dependence upon material thickness, as can be seen in Fig. 2. Unprocessed samples, with flat and smooth parallel faces were pressed into stacks after having been individually cleaned. An exponential fit (all with $R^2>0.95$) at each individual frequency leads to α for the corresponding frequency. Fabry-Perot resonances are addressed by only using the transmission maxima and interpolating between them in the valleys caused by the resonances. In theory, this could result in the loss of information, e.g. absorption peaks, but as the spacing between resonances is approx. 15 GHz, as can be seen in Fig. 1, and the resonances occur at different frequencies for each thickness, this possibility can be neglected. α is found to be 0.4 ± 10% cm^{-1} for Shapal at frequencies around 1 THz, which is consistent with the previously reported values for AlN and BN individually [9]. The attenuation of CeramAlOx is determined in the same way to be ~1.8 ± 10% cm^{-1}, which is consistent with the values for alumina [10]. All measurements were taken in an environment

Optical Materials EXPRESS

maintained at standard temperature and pressure conditions: 21°C, 75% RH. Samples were placed in an oven at 100 °C for one day at reduced pressure (<0.1 Bar) to remove any humidity within and measured directly afterwards. A second measurement after storing the samples at the previously mentioned ambient conditions for several days did not show any differences in transmission and thus, despite being hydrophilic like most ceramics, the water content absorbed in the material appears to be neglectable.

A home-built THz-TDS system was used for an initial broad-band characterization to give an impression of the material performance at higher frequencies, but as THz-TDS has a larger uncertainty for low attenuation coefficients [16,18] the full characterization was only conducted with the THz VNA.

Table 1. Composition and material properties of the ceramic materials under test and other ceramics and THz optical materials from literature.

(Trade) Name	Composition	Machinable	Refractive Index (n)	Loss Coefficient (α@1 THz) [cm^{-1}]
Shapal	71-74% AlN, 26% BN, various impurities [19]	Yes	~2.65	~0.4
Macor	46% SiO_2, 17% MgO, 16% Al_2O_3, 10% K_2O, 7% B_2O_3, 4% F [20]	Yes	NA	>30
CeramSil-C	SiC	No	NA	>20
CeramAlOx	Al_2O_3	No	~3.1	~1.8
Alumina from [10]	See reference	No	~3	~1
Boron Nitride from [9]	Various, see reference	No	~1.97-2.15	1-3
Aluminium Nitride from [9]	See reference	No	~2.92	~0.5
Low-loss polymers from 21]	See reference	Yes	~1.45-1.6	~0.5-2
HRFZ silicon from [1]	See reference	No/limited	~3.42	<0.05

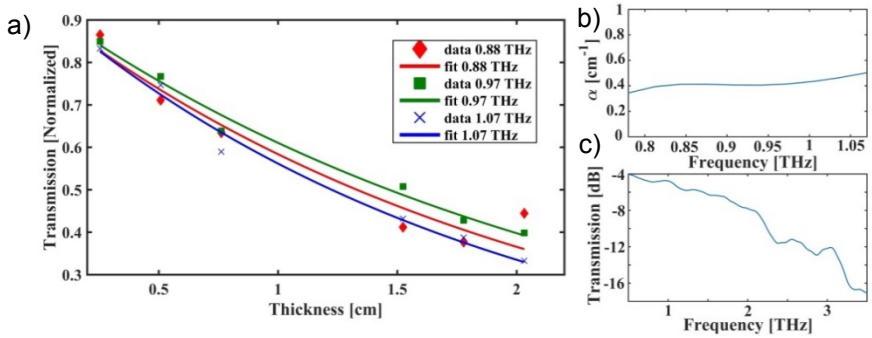

Fig. 2. Left: Signal attenuation at three different frequencies, plotted against material thickness allows extraction of the attenuation coefficient, shown at Top Right, from exponential fit lines. Bottom Right: The broadband THz-Time-Domain Spectroscopy scan shows little attenuation to well beyond 1 THz.

3. Micromachining of optical components

Initial starting points for machining parameters for larger features (>1 mm) for Shapal can be obtained from the data sheets of the material [19,20] and tooling, but no information is available about machining with tools in the order of tens or hundreds of microns, as is required for THz optics and photonic applications. Micro-milling can be used to realize micro-structured components such as Fresnel lenses. Due to the higher refractive index, the components can be thinner than comparable ones made from plastic.

To demonstrate the shaping capabilities of Shapal, we machined a continuous Fresnel lens with a nominal diameter of 11.2 mm on top of a 12.7 mm thick slab that focuses the incident THz radiation to the bottom face of the slab. Finite-difference time-domain (FDTD, software:

Optical Materials EXPRESS

Lumerical) simulations using the measured material properties show a −3 dB focal spot of around 190 μm width in the design, as shown in Fig. 3. The lens was designed using the lensmaker equation for a hemispherical lens and a modulus was used to introduce a step size of 198 μm [22]. The simulations were conducted as a 2D simulation because a 3D simulation of the full-scale component requires significant computational resources. To account for the effect of polarization, the polarization of the incident radiation was rotated by 180° in 1° steps and the electric field summed up. Perfectly matched layers were used as boundaries.

Table 2. Machining operations for Fresnel lens prototyping. The machine uses a spindle speed of 40,000 RPM, a feed rate of 30 mm/min and has a compressed air/low viscosity mineral oil/WD-40 mist as coolant.

Step	Description	Tool Diameter (mm)	# Tools Used	Axial Depth of Cut Increment (mm)	Stepover
0	Bed pocket	3.0000	1	—	—
1	Roughing horizontal raster	0.2032	2	0.300	0.9D = 0.183 mm
2	Roughing vertical raster	0.2032	2	0.300	0.9D = 0.183 mm
3	Roughing waterline	0.0760	1	0.050	0.6D = 0.046 mm
4	Finishing waterline	0.0300	3	0.015	0.45D = 0.014 mm

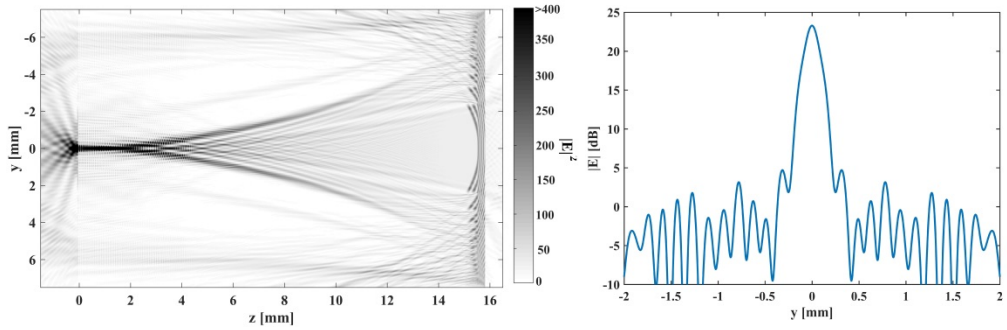

Fig. 3. Left: FDTD simulation shows that the THz radiation, coming from the right, propagates along the z-axis and is focused at the bottom of the structure on the left. Right: A planar slice of the electric field intensity 50 μm below the surface shows a −3 dB focal spot width of 190 μm.

First, a pocket was created in a sacrificial bed on a bespoke 3-axis micro-milling machine, to which the stock material was firmly attached. A coordinate system was established and the operations in Table 2 were performed. All operations used a 12° spiral lead in, where appropriate, to reduce thrust forces during plunges and prevent tool breakage. Spindle speed was fixed at 40,000 RPM, with a feed rate of 30 mm/min. All tools used were endmills, due to an unavailability of economical ballnose/bullnose cutters, at the detriment of surface finish of the lens. Finishing toolpaths were machined with Zecha 596.030.0003 endmills. The results are presented in Fig. 4. Surface finish and uniformity of the finished lens structure would be improved by being performed on a machining center equipped with a rotary axis to tilt the tool and another to spin the lens, however it serves as a demonstration of a realizable prototype manufactured with a general-purpose machine.

Optical Materials EXPRESS

Fig. 4. Scanning electron micrograph of a prototype Shapal Hi-M Soft Fresnel lens.

The Fresnel lens was then cleaned and characterized using the THz vector network analyzer in the following configuration: the radiation from the transmitting antenna is collimated with an off-axis parabolic mirror and directed towards the lens. The receiver is mounted on an xyz stage assembly and scans the planes perpendicular to the beam direction. The receiver's horn antenna has a 3 dB half angle of 10° and a beam waist radius of 0.66 mm, therefore the effective minimum detector size is ~1.3 mm. A scan of the xy plane at the front face of the lens serves as a reference. To find the focal spot, multiple xy scans were taken with a z-step of 300 µm, starting at the bottom face of the lens. The focal spot is determined by measuring the extrapolated average diameter of the 3 dB attenuation contour line. The scan shown in Fig. 5 shows the smallest measured focal spot and was captured with an xy step size of 300 µm at a distance of 1.2 mm from the sample surface. Nevertheless, the focal spot is measured to have a diameter around 200 µm which is in good agreement with the simulations, with the only discrepancy being that we found the focal spot at a distance of 1.2 mm from the surface rather than directly below the surface, which can be attributed to an incomplete removal of material. Each valley theoretically tapers to zero width at the root of a ring, however the tool occupies a finite width. As the attenuation of the 12.7 mm thick block of Shapal is ~5 dB and the measured intensity is approx. –2 dB in the focal spot corresponding to a net-gain of almost 3 dB in intensity.

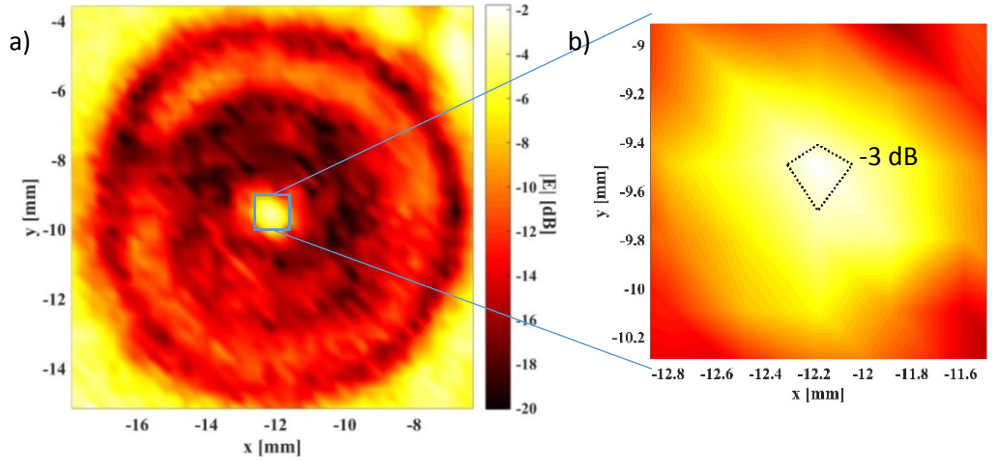

Fig. 5. a) The measured intensity in the xy-plane, 1.2 mm below the lens' back face. b) Zoom into the center shows a –3 dB focal spot size of around 200 µm in width.

The most challenging machining conducted was the drilling of 100 µm diameter holes to a depth of 1.3 mm to define photonic crystal type structures operating at 1 THz. The drilling operations required many pecking cycles, to facilitate chip removal at the extreme aspect ratio of 13. As seen in the micrographs in Fig. 6 the machining produces a good finish with no

Optical Materials EXPRESS

cracks, permitting the placement of holes with the high packing density required for photonic crystals. Thin walls of just 25 µm separate the holes. As can be seen in the zoomed-in micrograph (Fig. 6, Right) the side walls of the holes are smooth with the visible roughness originating from the grains of the ceramic material. This is, therefore, the best achievable surface finish. Since the grain size is less than 1% of the wavelength at 1 THz this will have no influence on the performance of the components.

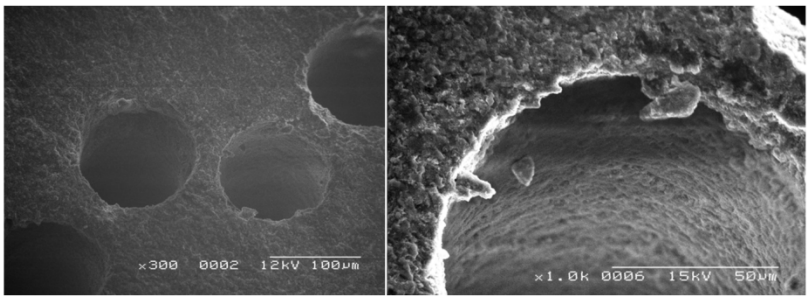

Fig. 6. Left: Micrograph from an array of holes on a hexagonal lattice suitable for use as a THz photonic crystal. The thin sidewalls with no cracks on the surface show the high packing density required for photonic crystals, is possible. Right: Zoomed micrograph on the second hole from the right. The smooth sidewalls show the grain structure of the material and no machining marks are visible, proving the surface finish is of suitable quality for THz photonic components.

4. Traditional bulk components: ceramic prism

For many optical components, such as lenses, the absorption of a material does not have a great impact on the performance of components as the optical path length (OPL) is only a few mm. This changes for bulk components, such as prisms, that often require an OPL in the order of cm. This means that the performance of the components is heavily impacted by material losses which is one of the reasons why standard optical components are still not as ready available for THz frequencies as they are for other parts of the spectrum. While prisms made from polymers such as PTFE do have a low enough absorption coefficient [21], their low refractive index results in a small operational range of angles and makes them less suitable for certain applications, such as prism coupling to plasmonic devices. The isosceles prism used in the following experiments has a base length of 25 mm and a vertex angle of 90°. This prism is intended for Attenuated Total Reflection (ATR) measurements and, therefore, the incoming beam reflects from the base at most incident angles, thus most standard prism characterization methods, e.g. measuring the minimum deviation angle, are impossible. As the requirements for a prism, i.e. its size, and, therefore, the optical path length, are highly dependent on the application, we demonstrate the dispersion to show the function of the prism. The measurements have been conducted with the THz VNA in an angular setup, where the incident beam is kept at a fixed angle and the exit angle is scanned in 0.1° steps to find the maximum transmission for the respective frequency. The incident, collimated beam has a diameter of 5 mm and a slot aperture with a width of ~2 mm is used on the receiving side to increase the angular resolution. Figure 7 shows that over a range of 0.78–1.07 THz there is only an angular difference of 1.3°, which reflects the low dispersion of the material. The data of the xy-plane scans, as shown in Fig. 5 and the simulation file used to extract the data in Fig. 3 can be found at: doi:10.15128/r23f4625432.

Optical Materials EXPRESS

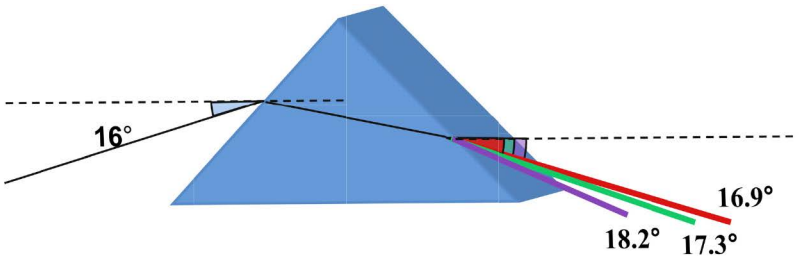

Fig. 7. Schematic of the measured dispersion of the prism with the different refraction angles for 0.78 THz (red), 0.92 THz (green) and 1.07 THz (purple) indicated. The overall measured deflection through dispersion in the frequency range is very low with only 1.3° difference.

5. Conclusion

We tested multiple low-cost ceramics for their use as optical materials at THz frequencies. Shapal, an AlN and BN based ceramic, exhibits the lowest losses of the tested materials and additionally has vast shaping capabilities as it is a machinable ceramic. It has the potential to fill the gap between low performance plastics and the high performance, but very expensive, HRFZ-Si, as a material of choice for THz optics. The micro-machining of a Fresnel lens is demonstrated and the drilling of holes for photonic components in the ceramic is discussed. A ceramic prism, as an example for a bulk optical component, has been presented.

Funding

FP7 People: Marie-Curie Actions (PEOPLE) NOTEDEV ITN (607521); Engineering and Physical Sciences Research Council (EPSRC) (EP/M506321/1).